The Cryosphere Discuss., 7, 3261–3291, 2013
www.the-cryosphere-discuss.net/7/3261/2013/
doi:10.5194/tcd-7-3261-2013

The Cryosphere Discussions
Open Access

Estimation of volume changes of mountain glaciers from ICESat data: an example from the Aletsch Glacier, Swiss Alps

J. Kropáček[1,2], N. Neckel[2], and A. Bauder[3]

[1]Institute for Cartography, TU-Dresden, Helmholzstr. 10, 01062 Dresden, Germany
[2]Institute of Geography, University of Tuebingen, Rümelinstr. 19–23, 72070 Tübingen, Germany
[3]Laboratory of Hydraulics, Hydrology and Glaciology (VaW), ETH Zurich, Gloriastrasse 37–39, 8092 Zürich, Switzerland

Received: 25 April 2013 – Accepted: 29 May 2013 – Published: 2 July 2013

Correspondence to: J. Kropáček (jan.kropacek@tu-dresden.de)

Published by Copernicus Publications on behalf of the European Geosciences Union.

Abstract

Worldwide estimation of recent changes in glacier volume is challenging, but becomes more feasible with the help of present and future remote sensing missions. NASA's Ice Cloud and Elevation Satellite (ICESat) mission provides accurate elevation estimates derived from the two way travel time of the emitted laser pulse. In this study two different methods were employed for derivation of surface elevation changes from ICESat records on example of the Aletsch Glacier. A statistical approach relies on elevation differences of ICESat points to a reference DEM while an analytical approach compares spatially similar ICESat tracks. Using the statistical approach, in the upper and lower parts of the ablation area, the surface lowering was found to be from $-2.1 \pm 0.15\,\mathrm{m\,yr^{-1}}$ to $-2.6 \pm 0.10\,\mathrm{m\,yr^{-1}}$ and from $-3.3 \pm 0.36\,\mathrm{m\,yr^{-1}}$ to $-5.3 \pm 0.39\,\mathrm{m\,yr^{-1}}$, respectively, depending on the DEM used. Employing the analytical method, the surface lowering in the upper part of the ablation area was estimated as $-2.5 \pm 1.3\,\mathrm{m\,yr^{-1}}$ between 2006 and 2009. In the accumulation area both methods revealed no significant trend. The trend in surface lowering derived by the statistical method allows an estimation of the mean mass balance in the period 2003–2009 assuming constant ice density and a linear change of glacier surface lowering with altitude in the ablation area. The resulting mass balance was validated by a comparison to another geodetic approach based on the subtraction of two DEMs for the years 2000 and 2009. We conclude that ICESat data is a valid source of information on surface elevation changes and on mass balance of mountain glaciers.

1 Introduction

Worldwide rapid retreat of mountain glaciers has been reported by numerous authors for the previous few decades (Lemke et al., 2007). Glaciers in the European Alps lost 10–15 % of their volume in the first five years of this century (Haeberli et al., 2007). The retreat of mountain glaciers leads to shifts in the hydrological regime of many rivers

(Huss et al., 2010) with consequences for hydro-power industry, irrigation schemes, river navigation etc. The increased glacier runoff is often mentioned in relation to sea level rise which has been estimated at 1.8 ± 0.5 m in the 21st century (Raper and Braithwaite, 2005; Bindoff et al., 2007). Oscillation in ice volume, which depends on both temperature and precipitation, contains a climate signal because surface lowering reacts faster to climate oscillation than glacier extent (Oerlemans, 2001). Distributed measurements of glacier surface lowering are also essential for the parametrization of glacier run-off models (Huss et al., 2010).

Glacier volume changes are measured locally by physically demanding glaciological and hydrological methods. On the other hand, unbiased periodic measurements of space-born instruments can provide a regional overview about glacier volume changes by geodetic means. The ICESat mission, which was primarily dedicated to the observation of polar ice sheets, provides a promising dataset for this purpose. ICESat data records were already utilized for the estimation of volume changes of mountain glaciers for nearly inaccessible glaciers in the Himalayas (Kääb et al., 2012) using the Shuttle Radar Topography Mission (SRTM) DEM as an elevation reference.

1.1 Objectives

This study is focused on a single glacier with good accessibility and availability of detailed DEMs, reliable climate data and other auxiliary datasets. Here we compare two methods to derive glacier elevation changes from ICESat data. The first method makes use of a reference DEM to which ICESat measurements are compared, while the second method utilizes only those parallel ICESat tracks that follow spatially similar ground tracks. For the first method we employed different elevation datasets and analyzed their influence to the accuracy of the derived surface lowering rates. The derived trends in surface elevation were validated by in-situ Differential Global Positioning System (DGPS) measurements and the mass balance estimates were compared to another method based on the subtraction of two DEMs. Further, we investigated the influence of topography and seasonal snow cover on the estimated surface elevation differences and their accuracy.

1.2 Description of Aletsch Glacier

Aletsch Glacier (Grosser Aletschgletscher) is an ideal test site since it represents the largest ice mass in the Alps and it is the only large glacier in the Alps with a good coverage of ICESat data. A rich archive of glaciological records and climate data date back to 1846 when the first ablation measurements on this glacier were carried out. Aletsch Glacier is located in the Bernese Alps in the central part of Switzerland. The accumulation area is on the southern slopes of the main mountain range, marked by the two prominent summits more than four thousand meters high: Jungfrau and Mönch. The common tongue is formed by the confluence of three tributaries (Grosser Aletschfirn, Jungfraufirn and Ewig Schneefeld) at the so called Concordia. From here the glacier flows first towards the SE and turns to the SW in a smooth bow. Aletsch Glacier is the longest (22.6 km) and largest (81.7 km^2) glacier in the European Alps and reaches an ice thickness of 890 m in its central part (Thyssen et al., 1969). The glacier has been retreating since the Little Ice Age; its volume loss has been estimated to -4.8×10^9 m^3 in the period from 1880 to 1999 (Bauder et al., 2007).

2 Data

2.1 ICESat/GLAS data

The GLAS on-board ICESat is a two channel instrument with a 1064 nm channel for surface altimetry and dense cloud heights, and a 532 nm channel for the investigation of vertical distribution of clouds and aerosols. Measurements are acquired in nadir every 172 m with a footprint diameter of 70 m (Schutz et al., 2005). The instrument was operational in the period 2003–2009. The launch of ICESat-2 with an improved instrument is planned for early 2016. Data acquisitions were carried out every 3 to 6

TCD
7, 3261–3291, 2013

months during 18 one-month campaigns. In the ideal case of no cloud cover, each campaign typically resulted in one repeat-pass track for a glacier. In this study we employed the ICESat/GLAS product L2 Global Land Surface Altimetry Data, release 33 (Zwally et al., 2003) denoted as GLA14, provided by the National Snow & Ice Data Center (NSIDC). The GLA 14 product contains information on land surface elevation, geolocation, reflectance as well as geodetic atmospheric and instrument corrections. Glacier outlines from 1998 are available via Global Land Ice Measurements from the Space (GLIMS) database (Armstrong et al., 2005) and were used for the selection of ICESat footprints on the glacier.

2.2 ICESat coverage of Aletsch Glacier

Aletsch Glacier is crossed by one nominal ICESat track which yields fourteen ground tracks out of which one track provides only sparse measurements. The ground tracks run in parallel in a stripe of 1.37 km width. This is a common situation in mid-latitudes between 59° S and 59° N for which the precision spacecraft pointing control was not used and the measurement points typically remain within 1 km distance from the reference orbit ground track (NSIDC, 2012). The ground tracks cross the glacier in three separate areas (Fig. 1, Table 1). The first area called Ewig Schneefeld denoted here as A1 belongs to the accumulation area of the glacier. The second area is located in the relatively flat confluence region of four tributary glaciers called Concordia (A2) which belongs to the ablation area of the glacier. The area covered by ICEsat measurements is relatively flat in its central part (mean surface slope of 2.7°) but becomes steeper toward the North. Concordia is crossed by a number of crevasses and by distinct medial moraines. The third area covered by ICESat measurements is located close to the terminus (A3) some 1600 m lower than the highest ICESat measurements of area A1. These three areas (A1, A2 and A3) which represent different units in terms of slope, surface roughness and glacier dynamics were treated separately.

TCD

7, 3261–3291, 2013

2.3 Digital elevation models

2.3.1 SRTM DEM

The Shuttle Radar Topography Mission (SRTM) conducted in February 2000 provided the geoscience community with two high resolution digital elevation models (Rabus et al., 2003; Farr and Kobrick, 2000). The data were acquired at C- and X-band during an 11 days mission and were interferometrically processed by the National Aeronautics and Space Administration (NASA) and the German Aerospace Center (DLR). The homogeneous freely available DEMs cover the entire land mass of the Earth between latitudes 60° N and 57° S. However the SRTM-X DEM was acquired with a swath width of 45 km leading to larger data gaps (Rabus, 2003). Due to the gaps between the acquisition stripes, the SRTM-X DEM is only available for area A3. In this study, we use the SRTM-C DEM version 3 which is available via the US Geological Survey (USGS) with a grid posting of 90 m and the SRTM-X DEM which is available via the German Aerospace Center (DLR) with a grid posting of 25 m. The vertical accuracy of the SRTM-C DEM as specified in the mission requirements is ±16 m at the 90 % confidence (Sun et al., 2003). It has been repeatedly confirmed that these requirements were met (Hoffman and Walter, 2006; Gorokhovich and Voustianiouk, 2006). Carabajal and Harding (2005) found a good match when comparing the SRTM DEM with ICESat points in an area in the Western United States. However for high altitudes SRTM elevations were found underestimated by up to 10 m by Berthier et al. (2006) in comparison with DEMs based on SPOT5 stereo-pairs and aerial photographs. Further, Gorokhovich and Voustianiouk (2006) showed that the error of the SRTM values have a strong correlation with slope and aspect, particularly for slope values higher than 10°.

2.3.2 ASTER GDEM

The Advanced Spaceborne Thermal Emission and Reflection Radiometer Global Digital Elevation Model (ASTER GDEM) covers the entire land mass of the World with a resolution of 30 m. It was produced by feature matching techniques using optical stereo-pairs acquired by nadir- and after-looking infrared cameras of the ASTER instrument on-board the Terra Satellite between 2000 and 2010. Multiple stereo pairs were processed for each point. The vertical accuracy is a function of the number of used stereo pairs and is specified as 17 m at the 95 % confidence level. For Aletsch Glacier, between 4 and 19 stereo-images were employed. A visual comparison of hill shading calculated from GDEM version 2 with high resolution DEMs revealed that GDEM over Aletsch Glaciers contains a high level of noise (Fig. 2) which corresponds to findings of Frey and Paul (2012). To account for the noise we used a smoothed version obtained by a 5 × 5 low pass filter besides the original dataset.

2.3.3 Airphoto DEM

This model was derived from aerial photographs from 1999 and 2009 by means of digital stereo-photogrammetry. A two phase procedure with automatic terrain extraction and manual post-processing for blunder elimination was applied. As a ground control 50 permanently marked geodetic points were used. The resulting DEM covers the glacier and its immediate surroundings and has a spatial resolution of 25 m. The expected accuracy is on the order of < 0.3 m which was confirmed by a cross validation using independent identical points outside the glacier.

3 Methods

3.1 Approach based on the elevation difference to a reference DEM

In order to make ICESat elevation measurements comparable between the non-identical tracks on the tilted and irregular shaped glacier surface, this method makes use of a static elevation reference. Therefore the surface elevation for each ICESat point was extracted from existing DEM data using bilinear interpolation of the four closest cells in the DEM following Carabajal and Harding (2005). The elevation difference between both datasets (ICESat – DEM) is defined as ΔH.

First of all the DEMs had to be checked for a horizontal shifts with respect to the ICESat profiles. Following Nuth and Kääb (2011) all ΔHs in off-glacier regions were normalized by the local slope inclination and were plotted against the terrain aspect. The horizontal shift was estimated by the amplitude of a fitted sinusoid and then removed by an adjustment of the reference coordinates of the DEMs (Table 2). The Airphoto DEM did not provide enough ΔH values for the fitting as it is limited mainly to the glacier area. Its shift with respect to the ICESat measurements could be derived by calculating the displacement between the Airphoto DEM and the adjusted SRTM-C DEM (Table 2).

Since the ICESat data is referenced to the TOPEX/Poseidon ellipsoid (Schutz et al., 2005) the first step was a conversion to WGS-84 heights following Bhang et al. (2007) and Wesche et al. (2009). In the next step, the ellipsoidal elevations were recalculated to heights above EGM96 geoid using information on geoidal heights contained in the GLA14 records.

For further analysis, only the ICESat measurements that meet the following criteria were used. First a threshold of vertical distance to the reference DEM of 100 m was applied. This threshold appears to effectively sort out all measurements affected by clouds. Since the vertical error of ICESat elevations increases with the incidence angle between the laser vector and the surface normal (Carabajal and Harding, 2005), it is reasonable to set an upper limit of slope of the glacier surface. A threshold of slope 10°, which was found critical by Hilbert and Schmullius (2012), was applied. This slope corresponds to a maximum elevation difference of 12.3 m within one footprint, assuming constant slope. To exclude the influence of a systematic bias in the ICESat data (differences between the lasers used during different ICESat campaigns, instrument drift, etc.) off-glacier measurements from the surrounding area were checked for a possible trend.

TCD
7, 3261–3291, 2013

3.1.1 Estimation of trends

In order to estimate trends in surface elevation change, a linear regression was fitted through all ΔH values per ICESat track and area. The statistical significance of the estimated trends was checked with an f test and the error of the regression was shown by its standard deviation. Irregularities in glacier surface changes caused by variation in albedo, debris cover and glacier flow together with processing artifacts of the DEM introduce a noise to the derived values of ΔH. The disturbing effect of noise is partially suppressed by a compensation of positive and negative deviations. On the other hand the variation of ΔH along the tracks can indicate the quality of the reference data set. A low variation indicates a good match between the ICESat profiles and their vertical projection on the DEM. Various DEMs were used as a reference and were compared in terms of variation of ΔH for all three areas.

3.1.2 DGPS measurements of the ICESat footprints

In order to get unbiased ground reference data, elevations of ICESat footprints were re-measured by Differential Global Positioning System (DGPS) measurements during a four day field campaign in July 2012 at Concordia. Since no geodetic point was reachable from the glacier without a loss of phase lock, the measured elevations are relative to the elevation of a base station placed on stable terrain next to the glacier. Elevations of 57 % of the footprint center points in area A2 were obtained with a relative accuracy on the order of centimeters. In order to provide a comparison with the DEMs, the DGPS measurements were used as the elevation reference and values of ΔH were calculated for each point.

3.1.3 Accounting for depth of seasonal snow cover

Seasonal snow cover introduces a variation into the time series of glacier elevations measured by ICESat. Snow depths are measured at two ground stations in the vicinity of the glacier: Eggishorn Station (2495 m a.s.l.) which is located 1.7 km to the SE from the lower part of the Aletsch Glacier and Belalp Station (2556 m a.s.l.) which is only about 4 km to the west from the terminus (Fig. 1). Unfortunately the Belalp Station has only been in operation since 2009. Snow depths for all dates of ICESat overpasses from Eggishorn Station are available. For the correction of ICESat elevations, we used the snow depths for days of ICESat flyovers measured at Eggishorn Station. The snow depths were directly subtracted from the ICESat elevation measurements.

3.1.4 Estimation of the glacier mass balance

The trends derived for the three areas were distributed along the elevation range of the glacier using a linear regression. In the next step, the interpolated trend in elevation bands of 100 m was multiplied by the area delimited by the elevation range of each band. The glacier mass balance in the ablation area was then obtained by summing up these volumes and multiplying by the estimate of the ice density, 900 kg m^{-3} (Bader, 1954). The error of the mass balance was quantified as a combination of the following contributions: error of derived trends, uncertainty of the glacier outlines and the error of the ice density.

To validate the results, the mass balance was calculated using another geodetic method based on the subtraction of two DEMs produced by aerial stereo-photogrammetry. For this purpose the Airphoto DEM for 2009 and a similar DEM for year 1999 (Bauder et al., 2007) were co-registered, re-sampled to the same spatial resolution (25 m) and subtracted from each other. The resulting volume was converted to mass balance using an assumption about the ice density. Thickness change was then calculated in elevation bands of 100 m and plotted against elevation. The following error estimation employed uncertainty of the elevation difference of the two DEMs, error of the ice density and uncertainty of the glacier outlines. The uncertainty of the elevation difference of the two DEMs was calculated after Koblet et al. (2010) using statistics of an off-glacier area calculated from each twentieth pixel in the sample in order to account for the autocorrelation inherent to the stereoscopically derived DEMs.

3.2 Approach based on the elevation difference between close tracks

Some ground tracks lie very close to each other so that they virtually follow the same profile of the glacier surface. Such pairs of tracks allow a comparison of measured elevations between two ICESat flyovers, independent of any elevation reference. The ICESat footprints in most cases do not have the same position along the nominal track since point measurements are not synchronized in the along-track direction. The relative elevation change between the close tracks in the pair can be obtained by calculating the vertical differences between the footprints of one track and their counterparts interpolated between points of the neighboring track. Then the mean of these differences represents an estimate of the absolute surface lowering between the two dates and the standard deviation of the differences provides an estimation of its error.

Close tracks were identified in a matrix of mutual distances between all possible pairs. Only the pairs separated by a maximum of 17 m were selected. This distance corresponds to a mutual overlap of two ICESat footprints of 70 %. In the next step all tracks with time separation of less than 12 months were excluded. Correction for the height of the seasonal snow was applied beforehand by the snow depths measured at Eggishorn. Surface lowering between the dates in the selected pairs was calculated separately in each area.

4 Results

4.1 Trends in surface elevation derived from ICESat using a reference DEM

The surface lowering of Aletsch Glacier observed from ICESat elevations appears close to zero in the accumulation area (A1). The lowering in the upper part of the ablation area (A2) is 2.2 $\mathrm{m\,yr^{-1}}$ and it increases towards the terminus (area A3) where it becomes about twice as much (Tables 3–5, Fig. 3). This is a common pattern observed at alpine glaciers in the last decade (Huss et al., 2008; Bauder et al., 2007;

Haberli et al., 2007). The analysis of ΔH for the surrounding area not covered by the glacier did not produce any significant trend, which confirms that the use of different lasers for the ICESat campaigns or a possible instrument drift did not affect the trends extracted for Aletsch Glacier.

4.1.1 Area A1

In area A1, which is located in the accumulation part of the glacier, no statistically significant trend in surface elevation change was revealed from the ICESat records (Table 3). The best results in terms of variation of ΔH is achieved when using the Airphoto DEM. When comparing the two global DEMs, the variation in ΔH is much lower for the SRTM DEM than for the ASTER GDEM. This indicates a good performance of the InSAR technique in terrain reconstruction in snow covered areas with lack of features for stereo-processing. Noise which is present in the ASTER GDEM in the areas covering glaciers leads to a truncation of 76.1 % of measurements which improves when using the smoothed data but the standard deviation of ΔH stays rather high. It appears that the GDEM is less suitable for ice surface analysis in the accumulation area than the DEMs created by SAR interferometry and aerial stereoscopy.

4.1.2 Area A2

The statistically significant trends derived for Concordia based on the ICESat measurements range from -2.1 ± 0.15 to $-2.6 \pm 0.10\,\mathrm{m\,yr^{-1}}$ depending on the DEM used as an elevation reference (Table 4). Ground measurements of the surface elevation of the ICESat footprints during the summer of 2012 using DGPS confirm the results achieved using the reference DEMs. If the GPS altitudes are taken as the elevation reference we obtain a trend that amounts for $-2.6 \pm 0.08\,\mathrm{m\,yr^{-1}}$ which is identical to the trends based on the Airphoto DEM (Table 4).

The estimation of surface lowering in this area benefits from long intersections of ICESat tracks with the glacier surface. The smooth surface topography leads to a relatively low variation of ΔH, which reaches only 1.9 m in the case of the Airphoto DEM. This confirms its good quality over the ablation area, which provides plenty of distinct features for stereoscopic processing based on feature matching. Smoothing of the ASTER GDEM improves the variation of ΔH but does not affect the trend significantly. The trends derived using the ASTER GDEM slightly underestimate the rates of the surface lowering, taking the DGPS measurements as a reference, while the use of the SRTM-C DEM leads to a good match. These results prove usefulness of ICESat data for the estimation of surface lowering rates.

4.1.3 Area A3

Statistically significant trends in surface lowering were derived from ICESat data for area A3 using four different DEMs. The estimated surface lowering is higher with respect to area A2 and ranges from -3.3 to $-5.1\,\mathrm{m\,yr^{-1}}$ depending on which DEM was used (Table 5). The best performance in terms of variation in ΔH was achieved when using the Airphoto DEM but the trend differs from the trends provided by DEM from spaceborne platforms. Both the trend and the variations in ΔH are almost identical when comparing the SRTM-X DEM with the SRTM-C DEM. A very similar value of trend and ΔH variation was achieved for the ASTER GDEM. In this area, the comparison of the different DEMs is indeed affected by changes of the surface geometry between different acquisition dates taking into account the high dynamics of the retreating glacier terminus. Some ICESat measurements from winter acquisitions had to be canceled due to erroneous elevations caused by the presence of low clouds.

4.1.4 Estimation of mass balance

Since no significant trend was derived for the accumulation area, the distribution of the trend was limited entirely to the ablation area. It means that only trend values representing the area A2 and A3 were used for the linear fitting and that the elevation bands cover an altitude range from 1800 m a.s.l. to 3000 m a.s.l., the upper one being

TCD
7, 3261–3291, 2013

an approximate position of the equilibrium line. The mass balance calculation using an ice density of 900 $kg\,m^{-3}$ produced a total mass balance in the range from -0.077 ± 0.013 to $-0.091 \pm 0.015\,Gt\,yr^{-1}$ (Table 6). For the error estimation we assumed the accuracy of the ice density estimate to be 11 % which corresponds to the range of ice density estimates commonly used in glacier mass balance studies (Fischer, 2011). The accuracy of the glacier area delimited by the elevation bands and the GLIMS outlines was estimated to be 10 %.

The comparison of the mass balance calculated from ICESat measurements with the mass balance obtained by the subtraction of the Airphoto DEM and the SRTM-C DEM in the ablation area shows an overestimation of the former (Table 6). One reason for this is a relative overestimation of the surface lowering in the areas A2 and A3. Another reason is a non-linearity in the dependency between the surface lowering and the altitude found by the subtraction of the two DEMs. This can be seen in the profile constructed from mean values lowering in the altitude bands (Fig. 4). This non-linearity is not captured by the ICESat data due to the gaps in data coverage along the elevation range.

4.2 Surface lowering derived from the pairs of close tracks

For the area A1, two pairs of close tracks both with a temporal distance of about three years were identified (Table 7). They produced low values of surface lowering which are not significant when comparing it with the standard deviation of ΔH. The pair of close tracks identified in area A2 has a good time separation of 34 months and a high number of samples (17 measurements). The time span of this pair covers approximately the second half of ICESat's mission period. The use of the snow depth data leads to a trend which is very close to the one derived using the DGPS and also very close to the SRTM-C DEM. The pair of close tracks identified for the area A3 have a low time separation of around one year and contains only five pairs of points, but the tracks were all acquired at the end of the ablation season in October and November. The calculated surface lowering matches the trend derived using DEMs, although the standard devi-

TCD
7, 3261–3291, 2013

ation of ΔH is close to the value of the surface lowering. Although the close tracks do not cover the whole ICESat mission period, overall the trends derived match well to the trends based on a reference DEM. This suggests that this approach can provide useful results, especially in areas with limited availability of reliable terrain information.

5 Discussion

Aletsch Glacier has a unique position amongst the glaciers in the European Alps with respect to the ICESat mission. The glacier features a favorable coverage of ICESat data both in terms of number of tracks passing over the glacier surface and the distribution of the tracks over representative areas with a high relevance to the observation of mass balance. The intersections of the tracks with the glacier surface are long, especially in the case of Concordia (area A2) which allowed a robust statistic analysis of the altitude differences. Other glaciers in the Alps that are crossed by ICESat tracks have either a short intersection or are crossed by only a few tracks which does not allow a proper extraction of trends in surface lowering.

Ground DGPS measurements on Concordia provided an independent elevation reference which validates the results achieved by various DEMs. Even though there is a certain variation of ΔH present when using the DGPS data, it is lower than in the case of the DEMs. This residual variation can be attributed to terrain undulations in the ICESat footprints and probably also to the effects of the horizontal component of glacier movements. The trend for Concordia based on DGPS is equal to the one for the Airphoto DEM and very close to the one for the SRTM-C DEM. The trend derived for Concordia also corresponds remarkably well to the trend achieved in the close track approach.

The available DEMs that were used for the analysis clearly show differences in the level of detail, amount of noise and spatial coverage. The SRTM-C DEM provides a robust estimate of ΔH for all three areas. The penetration effect discussed by several authors (e.g. Rignot et al., 2001) did not affect the results since the accumulation area

TCD
7, 3261–3291, 2013

was treated separately. The spatially limited SRTM-X DEM does not seem to provide a better elevation reference than the SRTM-C DEM. The ASTER GDEM contains a high level of noise on the glacier surface that can be suppressed by application of a smoothing filter and it definitely has a lower quality in the snow covered accumulation area. The elevation reference provided by the Airphoto DEM is almost as accurate as the ground DGPS measurements.

The use of in-situ snow depth measurements allowed us to suppress a seasonal signal in the data and to avoid reduction of the dataset by a selection of measurements only from a certain season. The representativeness of a single snow depth measurement is biased by the spatial irregularity of precipitation and the redistribution of snow cover by wind. On the other hand, snow fall can occur at any time of the year in the high mountains which can indeed affect ICEsat elevations from a selected period.

The trend in glacier surface elevations derived from ICESat data corresponds overall to the results of another geodetic method based on subtraction of two DEMs from the years 2000 and 2009 and to a detailed reconstruction of mass balance by Farinotti et al. (2012). Certain overestimation of trends derived from ICESat measurements for areas A2 and A3 and a non-linearity of the surface lowering from the DEM subtraction lead to an overestimation of the mass balance (Fig. 4). The non-linearity represented by a distinct peak in the profile at the elevation around 2200 m a.s.l. is most likely due to the narrowing of the glacier bed from 1600 m to 960 m which constrains the glacier flow. It has to be noted, that different methods of mass balance estimation do not lead to identical results and that great care has to be taken when comparing them (Fischer, 2011). On top of that, in our case, the time period covered by the input data of the two methods is not identical.

6 Conclusions

The presented statistically significant trends in surface lowering derived from ICESat measurements for Aletsch Glacier which were further validated by employment

TCD
7, 3261–3291, 2013

of ground DGPS measurements show that ICESat data can provide robust information about changes in volume of mountain glaciers. The estimated mass balance was compared to another geodetic method based on the subtraction of two DEMs. These results for a single glacier confirm the reliability of regional estimates of mass balance of mountain glaciers based on ICESat data. It was shown that even if the use of global DEMs as elevation reference can lead to a realistic estimate of the surface lowering, the use of a higher quality DEM provides better results in terms of variation of ΔH which in turn leads to a higher significance of the estimated trends and to a more accurate mass balance. Global availability of a detailed high quality DEM in the future will indeed improve the accuracy of the derived mass balance of mountain glaciers. In this context, high expectations are pointed towards the global DEM derived from the data of the TanDEM-X mission. It appeared that the method relying on close tracks has many limitations imposed by the random distribution of the ICEsat tracks in time and space. It can nevertheless provide a valuable information for glaciers with no or low quality elevation data. The results for the Aletsch Glacier indicate that for a single glacier, even if the surface lowering is realistically assessed in several areas on the glacier, the calculated mass balance may be affected by local non linearity due to the dependence of the surface lowering on the elevation.

Acknowledgements. This work was supported by the German Research Foundation (DFG) Priority Programme 1372, "Tibetan Plateau: Formation – Climate – Ecosystems" within the DynRG-TiP ("Dynamic Response of Glaciers on the Tibetan Plateau to Climate Change") project under the codes SCHE 750/4-1, SCHE750/4-2, SCHE 750/4-3, and by the German Federal Ministry of Education and Research (BMBF) Programme "Central Asia – Monsoon Dynamics and Geo-Ecosystems" (CAME) within the WET project ("Variability and Trends in Water Balance Components of Benchmark Drainage Basins on the Tibetan Plateau") under the code 03G0804D. ICESat data was provided by NSIDC, SRTM-C DEM was obtained from the USGS and the SRTM-X DEM was provided by the DLR. ASTER GDEM is a product of METI and NASA. The field measurements of the snow depth were provided by the Institute for Snow and Avalanche Research in Davos, Switzerland. Aerial photographs for 1980 and 1999 were provided by the Federal Office of Topography (Swisstopo).

References

Armstrong, R., Raup, B., Khalsa, S., Barry, B., Kargel, J., Helm, C., and Kieffer, H.: GLIMS Glacier Database, National Snow and Ice Data Center, Boulder, Colorado, USA, 2005.

Bader, H.: Sorge's law of densification of snow on high polar glaciers, J. Glaciol., 2, 319–323, 1954.

Bauder, A., Funk, M., and Huss, M.: Ice-volume changes of selected glaciers in the Swiss Alps since the end of the 19th century, Ann. Glaciol., 46, 145–149, 2007.

Bhang, K. J., Schwartz, F. W., and Braun, A.: Verification of the Vertical Error in C-band SRTM DEM Using ICESat and Landsat-7, Otter Tail County, MN, IEEE T. Geosci. Remote, 45, 36–44, 2007.

Berthier, E., Arnaud, Y., Vincent, C., and Rémy, F.: Biases of SRTM in high-mountain areas: implications for the monitoring of glacier volume changes, Geophys. Res. Lett., 33, L08502, doi:10.1029/2006GL025862, 2006.

Bindoff, N., Willebrand, J., Artale, V., Cazenave, A., Gregory, J., Gulev, S., Hanawa, K., Le Quéré, C., Levitus, S., Nojiri, Y., Shum, C., Talley, L., and Unnikrishnan, A.: Observations: oceanic climate change and sea level, in: Climate Change 2007: the Physical Science Basis, Contribution of Working Group I to the Fourth Assessment Report of the Intergovernmental Panel on Climate Change, Cambridge University Press, Cambridge, UK and New York, NY, USA, 2007.

Carabajal, C. C. and Harding, D. J.: ICESat validation of SRTM C-band digital elevation models, Geophys. Res. Lett., 32, L22S01, doi:10.1029/2005GL023957, 2005.

Fischer, A.: Comparison of direct and geodetic mass balances on a multi-annual time scale, The Cryosphere, 5, 107–124, doi:10.5194/tc-5-107-2011, 2011.

Farinotti, D., Usselmann, S., Huss, M., Bauder, A., and Funk, M.: Runoff evolution in the Swiss Alps: projections for selected high-alpine catchments based on ENSEMBLES scenarios, Hydrol. Process., 26, 1909–1924, doi:10.1002/hyp.8276, 2012.

Farr, T. G. and Kobrick, M.: Shuttle radar topography mission produces a wealth of data, Eos Trans. AGU, 81, 583, doi:10.1029/EO081i048p00583, 2000.

Frey, H. and Paul, F.: On the suitability of the SRTM DEM and ASTER GDEM for the compilation of topographic parameters in glacier inventories, Int. J. Appl. Earth Observ. Geoinf., 18, 480–490, doi:10.1016/j.jag.2011.09.020, 2012.

Gorokhovich, Y. and Voustianiouk, A.: Accuracy assessment of the processed SRTM-based elevation data by CGIAR using field data from USA and Thailand and its relation to the terrain characteristics, Remote Sens. Environ., 104, 409–415, 2006.
Haeberli, W., Hoelzle, M., Paul, F., and Zemp, M.: Integrated monitoring of mountain glaciers as key indicators of global climate change: the European Alps, Ann. Glaciol., 46, 150–160, 2007.
Hilbert, C., Schmullius, C.: Influence of Surface Topography on ICESat/GLAS Forest Height Estimation and Waveform Shape, Remote Sens., 4, 2210–2235, 2012.
Hoffman, D. and Walter, J.: How complementary are SRTM-X and -C band digital elevation models?, Photogramm. Eng. Rem. S., 72, 261–268, 2006.
Huss, M., Bauder, A., Funk, M., and Hock, R.: Determination of the seasonal mass balance of four Alpine glaciers since 1865, J. Geophys. Res., 113, F01015, doi:10.1029/2007JF000803, 2008.
Huss, M., Jouvet, G., Farinotti, D., and Bauder, A.: Future high-mountain hydrology: a new parameterization of glacier retreat, Hydrol. Earth Syst. Sci., 14, 815–829, doi:10.5194/hess-14-815-2010, 2010.
Koblet, T., Gärtner-Roer, I., Zemp, M., Jansson, P., Thee, P., Haeberli, W., and Holmlund, P.: Reanalysis of multi-temporal aerial images of Storglaciären, Sweden (1959–99) – Part 1: Determination of length, area, and volume changes, The Cryosphere, 4, 333–343, doi:10.5194/tc-4-333-2010, 2010.
Lemke, P., Ren, J., Alley, R., Allison, I., Carrasco, J., Flato, G., Fujii, Y., Kaser, G., Mote, P., Thomas, R., and Zhang, T.: Observations: changes in snow, ice and frozen ground, in: Climate Change 2007: the Physical Science Basis, Contribution of Working Group I to the Fourth Assessment Report of the Inter-governmental Panel on Climate Change, Cambridge University Press, Cambridge, UK and New York, NY, USA, 2007.
NSIDC: available at: http://nsidc.org/data/icesat/orbit_grnd_trck.html (last access: 28 June 2012), 2012.
Nuth, C. and Kääb, A.: Co-registration and bias corrections of satellite elevation data sets for quantifying glacier thickness change, The Cryosphere, 5, 271–290, doi:10.5194/tc-5-271-2011, 2011.
Oerlemans, J.: Glaciers and Climate Change, A. A. Balkema Publishers, Rotterdam, 148 pp., 2001.

TCD
7, 3261–3291, 2013

Estimation of volume changes of mountain glaciers from ICESat data

J. Kropáček et al.

Rabus, B., Eineder, M., Roth, A., and Bamler, R.: The shuttle radar topography mission, a new class of digital elevation models acquired by spaceborne radar, Int. Soc. Photogramme., 57, 241–262, 2003.
Raper, S. C. B. and Braithwaite, R. J.: Low sea level rise projections from mountain glaciers and icecaps under global warming, Nature, 439, 311 –313, 2006.
Rignot, E., Echelmeyer, K. A., and Krabill, W.:, Penetration depth of interferometric synthetic-aperture radar signals in snow and ice, Geophys. Res. Lett., 28, 501– 504, 2001.
Schutz, B. E., Zwally, H. J., Shuman, C. A., Hancock, D., and Di Marzio, J. P.: Overview of the ICESat mission, Geophys. Res. Lett., 32, L21S01, doi:10.1029/2005GL024009, 2005.
Sun, G., Ranson, K. J., Kharuk, V. I., and Kovacs, K.: Validation of surface height from shuttle radar topography mission using shuttle laser altimeter, Remote Sens. Environ., 88, 401–411, 2003.
Thyssen, F. and Ahmad, M.: Ergebnisse seismischer Messungen auf dem Aletschgletscher, Polarforschung, Bremerhaven, Alfred Wegener Institute for Polar and Marine Research & German Society of Polar Research, 39, 283–293, 1969.
Wesche, C., Riedel, S., and Steinhage, D.: Precise surface topography of the grounded ice ridges at the Ekströmisen, Antarctica, based on several geophysical data sets, Int. Soc. Photogramme., 64, 381–386, 2009.
Zwally, H. J., Schutz, R., Bentley, C., Bufton, J., Herring, T., Minster, J. Spinhirne, J., and Thomas, R.: GLAS/ICESat L2 Global Land Surface Altimetry Data, Version 33, National Snow and Ice Data Center, Boulder, Colorado, USA, 2003.

TCD
7, 3261–3291, 2013
Estimation of volume changes of mountain glaciers from ICESat data
J. Kropáček et al.

Table 1. Characteristics of the test areas on Aletsch Glacier covered by ICESat footprints.

area covered by ICESat points	area ID	altitude range (m)	mean slope (deg.)	points per track
Ewig Schneefeld	A1	3350–3450	3.2	1–21
Concordia	A2	2600–3000	2.7–13.0	5–20
terminus	A3	1950–2200	4.2	2–13

TCD
7, 3261–3291, 2013

Table 2. Horizontal shifts of the reference DEMs with respect to the ICESat measurements which had to be removed before the extraction of ΔH values.

DEM	horizontal shift (m)	azimuth of the shift (deg.)
SRTM-C	70.8	124.2
SRTM-X	40.0	72.1
Airphoto DEM	55.1	−106.3
ASTER GDEM	17.1	200.6

TCD
7, 3261–3291, 2013

Table 3. Linear regression of ΔH revealed no significant change of surface elevation for area A1 (accumulation area).

elevation reference	No. Tracks	mean ΔH (m)	σ of ΔH (m)	trend ($\mathrm{m\,yr^{-1}}$)	f value	canceled points (%)	canceled tracks (No)
SRTM-C	13	8.1	4.7	-0.2 ± 0.32	0.41	55.8	1
ASTER GDEM original	13	−13.4	12.9	0.2 ± 1.05	0.02	76.1	2
ASTER GDEM smoothed	13	−12.7	10.2	0.1 ± 0.67	0.04	58.9	1
Airphoto DEM	13	5.5	3.9	-0.0 ± 0.30	0.02	54.3	1

TCD
7, 3261–3291, 2013

Table 4. Trends in glacier surface elevation for area A2 using different DEMs as elevation reference. All trends are statistically significant.

elevation reference	No. Tracks	mean ΔH (m)	σ of ΔH (m)	trend (m yr^{-1})	f value	canceled points (%)	canceled tracks (No)
SRTM-C	12	−6.1	2.8	-2.5 ± 0.13	380.6	14.9	1
ASTER GDEM original	12	−3.8	4.2	-2.2 ± 0.20	125.9	33.2	1
ASTER GDEM smoothed	12	−3.3	3.5	-2.1 ± 0.15	183.8	15.9	1
Airphoto DEM	12	10.7	1.9	-2.6 ± 0.10	759.8	16.8	1
DGPS	12	15.0	0.9	-2.6 ± 0.08	788.5	7.5	1

TCD
7, 3261–3291, 2013

Table 5. Trends in glacier surface elevation for area A3 using different DEMs as elevation reference.

elevation reference	No. Tracks	mean ΔH (m)	σ of ΔH (m)	trend ($\mathrm{m\,yr^{-1}}$)	f value	canceled points (%)	canceled tracks (No)
SRTM-C	11	−25.6	4.4	-5.1 ± 0.35	209.06	28.2	2
ASTER GDEM original	11	−18.2	4.6	-4.3 ± 0.52	68.32	56.4	2
ASTER GDEM smoothed	11	−17.1	4	-5.1 ± 0.34	217.44	30.8	2
Airphoto DEM	11	17	3.8	-3.3 ± 0.36	84.77	39.7	2
SRTM-X	11	−22.6	4.4	-5.3 ± 0.39	189.23	33.3	2

TCD
7, 3261–3291, 2013

Table 6. Mass balance of Aletsch Glacier estimated from ICESat measurements using different DEMs as elevation reference and from the subtraction of the DEMs for years 1999 and 2009.

DEM	mass balance ($Gt\,yr^{-1}$)
Airphoto DEM	-0.079 ± 0.014
SRTM-C	-0.091 ± 0.015
GDEM ASTER original	-0.085 ± 0.016
GDEM ASTER smoothed	-0.077 ± 0.013
subtraction of DEMs	-0.092 ± 0.029

TCD
7, 3261–3291, 2013

Estimation of volume changes of mountain glaciers from ICESat data

J. Kropáček et al.

TCD
7, 3261–3291, 2013

Estimation of volume changes of mountain glaciers from ICESat data

J. Kropáček et al.

Table 7. Trend in surface lowering estimated from the pairs of close tracks over the three areas.

area	date, track1	date, track2	same season	distance [m]	trend $m\,yr^{-1}$ (snow data)	trend $m\,yr^{-1}$ (no snow data)	time distance [months]	number of points	σ of ΔH
A1	29 May 2005	12 Oct 2008	no	1.0	−0.9	−0.9	41	7	3.2
A1	01 Jun 2006	17 Mar 2009	nearly	6.6	−0.1	0.4	34	5	1.5
A2	01 Jun 2006	17 Mar 2009	nearly	1.9	−2.5	−2.0	34	17	1.3
A3	02 Nov 2006	10 Oct 2007	yes	5.3	−4.4	−4.4	11	5	4.1

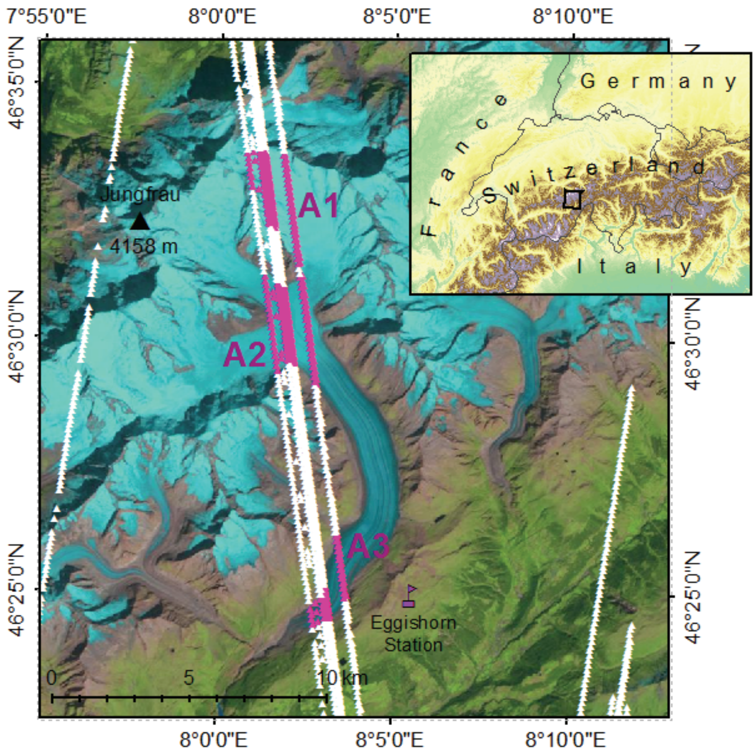

Fig. 1. Ground tracks of ICESat cross the surface of Aletsch Glacier in three separate places: Ewig Schneefeld (A1), Concordia (A2) and the lower part close to the terminus (A3). ICESat measurements on the glacier are highlighted in violet. In the background is a Landsat TM image from 28 August 2011.

TCD
7, 3261–3291, 2013

Estimation of volume changes of mountain glaciers from ICESat data

J. Kropáček et al.

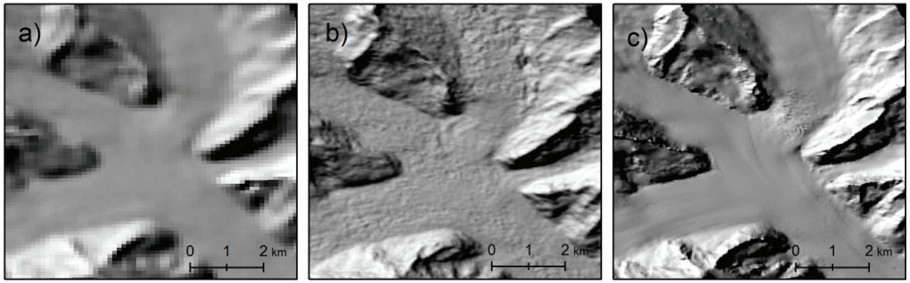

Fig. 2. The area A2 (Concordia) on different DEMs shown as hill shading. **(a)** The SRTM-C DEM features a smooth surface with little detail. Artifacts are clearly visible on the glacier surface in the case of the ASTER GDEM **(b)** while the Airphoto DEM **(c)** has a smooth surface with a distinct medial moraine.

TCD
7, 3261–3291, 2013

Estimation of volume changes of mountain glaciers from ICESat data

J. Kropáček et al.

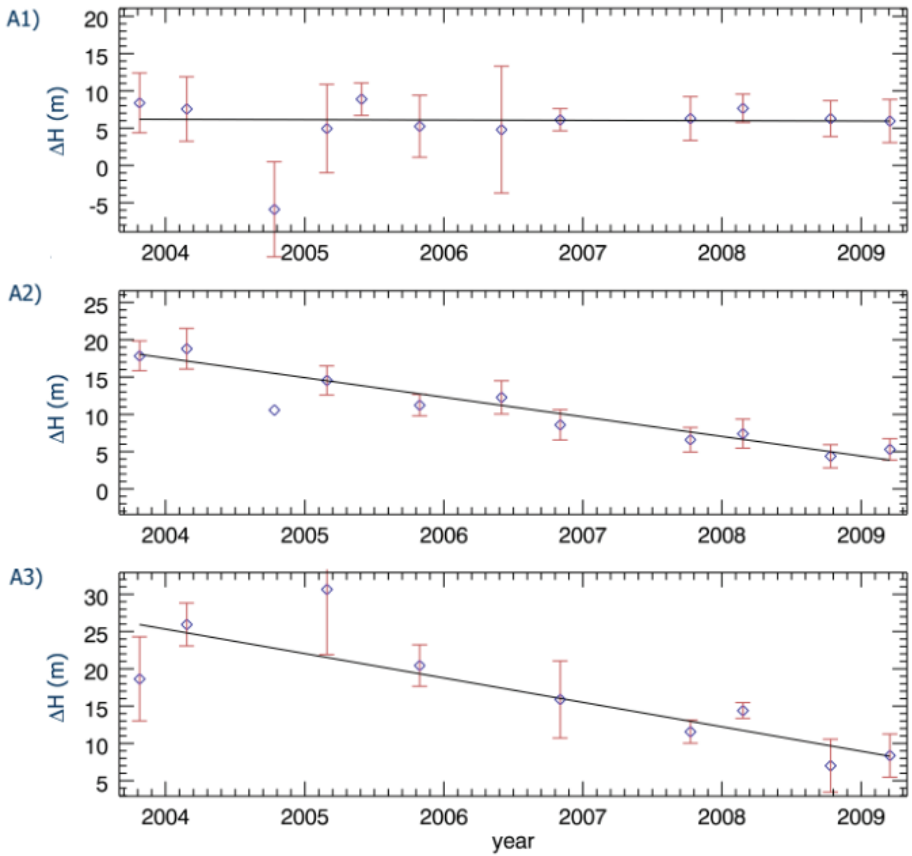

Fig. 3. Linear regression of ICESat measurements in areas A1, A2 and A3 using the Airphoto DEM as an elevation reference. The error bars show the standard deviation of ΔH in each ICESat track.

TCD
7, 3261–3291, 2013

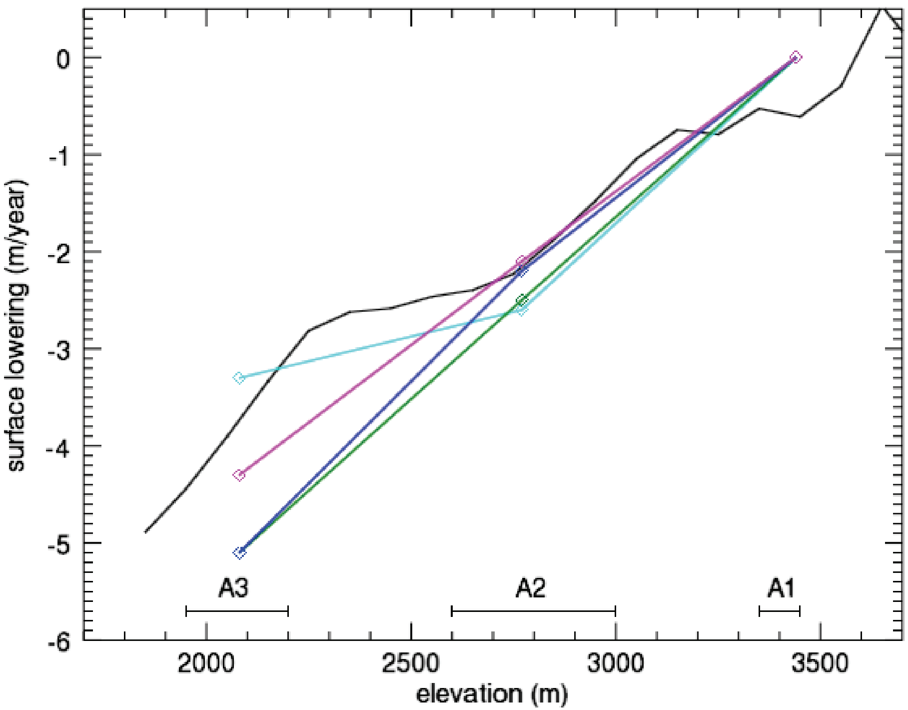

Fig. 4. Surface lowering in elevation bands of 100 m derived from the subtraction of two DEMs (black line) and surface lowering from ICESat measurements using the Airphoto DEM (cyan), SRTM-C DEM (green), the ASTER GDEM original (blue) and the ASTER GDEM smoothed (magenta). The elevation ranges covered with the ICESat data (A1, A2 and A3) are marked by horizontal lines in the lower part of the images.

TCD
7, 3261–3291, 2013